Electronic Supplementary Information

N/Si-codoped nanocrystalline diamonds as highly sensitive luminescent nanothermometers

Mabel Rodríguez-Fernández,[1] María Gragera,[1] Iván Carrillo-Berdugo,[1,*] Rodrigo Alcántara,[1] Paulius Pobedinskas,[2,3] Ken Haenen,[2,3] Gonzalo Alba,[4] David Zorrilla[1], Javier Navas[1,*]

[1] Department of Physical Chemistry, University of Cádiz, E-11510 Puerto Real, Spain.
[2] IMO-IMOMEC, Hasselt University, Wetenschapspark 1, 3590 Diepenbeek, Belgium.
[3] IMOMEC, IMEC vzw, Wetenschapspark 1, 3590 Diepenbeek, Belgium.
[4] Department of Science Materials and Metallurgic Engineering and Inorganic Chemistry, University of Cádiz, E-11510 Puerto Real, Spain.

*Corresponding author: Javier Navas (javier.navas@uca.es), Iván Carrillo-Berdugo (ivan.carrillo@uca.es)

S1. Input files for vibronic spectra simulations in Gaussian 16

Gaussian 16 input files related to this work are also accessible as Supporting Information in an additional .zip file. The contents of this file are here listed:

```
.
├── diamondoid.gjf
├── diamondoid-NV_ground.gjf
├── diamondoid-SiV_ground.gjf
├── diamondoid-NV_excited.gjf
├── diamondoid-SiV_excited.gjf
└── diamondoid-XV_fcht.gjf
```

S2. Analysis of the full width at half maximum from Raman spectra

From the Raman spectra registered for the nine samples of N/Si-codoped nanocrystalline diamonds, the full width at half maximum (FWHM) was estimated. The values obtained are shown in Figure S1. According to these values, all samples here studied exhibit similar crystallinity, as proven by a very narrow range of differences in the FWHM if the diamond Raman signal, within 6.3-9.2 cm^{-1}.

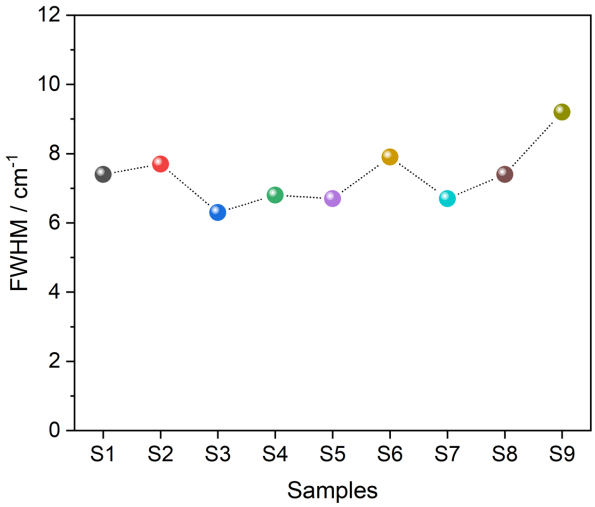

Figure S1. FWHM values extracted from the Raman spectra registered for the nine samples of N/Si-codoped nanocrystalline diamonds.

S3. Scanning electron microscopy

Scanning electron microscopy (SEM) images were obtained to observe the morphology of the surface of the N/Si-codoped nanocrystalline diamonds (NCD). As all the samples were grown under similar conditions, the morphology study was focused on the most interesting one for their application in luminescence nanothermometry (sample S8) and sample S5 for comparison purposes being representative of the rest of the samples. Figure S1 shows the SEM images for the samples S8 and S5. In both cases, well-faceted crystals were obtained, being the crystals of the sample S5 smaller than those of the sample S8. It is well-known that the effect of an increase of methane flow is a higher growth rate due to the fact that there are more carbon radicals in the surface. In the same way, when the reactant pressure and the microwave power increase, the growth rate also increases. As both samples were grown under the same microwave power (4500W), the effect of the methane flow and the reactant pressure on the nanocrystal size are analysed. The methane flow was higher in the case of the sample S5, thus, it could be expected that the nanocrystal size would be larger than the sample S8. However, the nanocrystal size of the sample S5 is smaller than that of the sample S8. This is due to the fact that the reactant pressure employed during the growth of the sample S8 was higher (60 Torr) than the one of sample S5 (50 Torr). Thus, in regard of the nanocrystal size, the increase of the pressure in 10 Torr is more determining than the decrease of the % C/H in 0.74%.

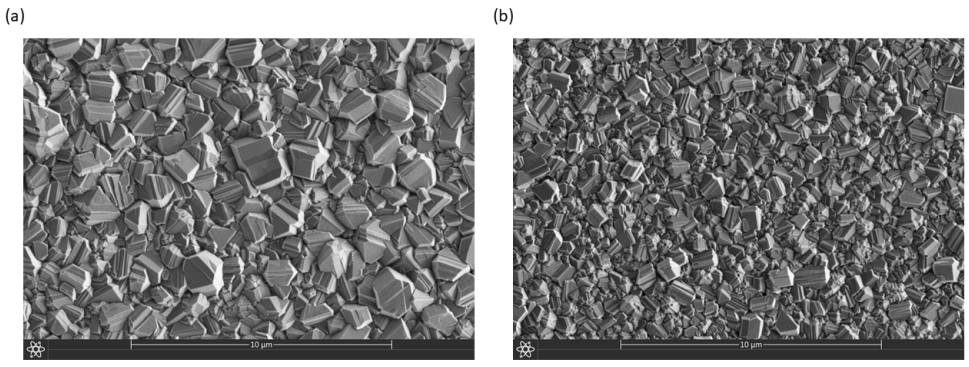

Figure S2. SEM images of the samples S8 (a) and S5 (b).

S4. SEM and cathodoluminescence (CL)

SEM and CL measurements show the expected results for N/Si-codoped nanocrystalline diamonds.

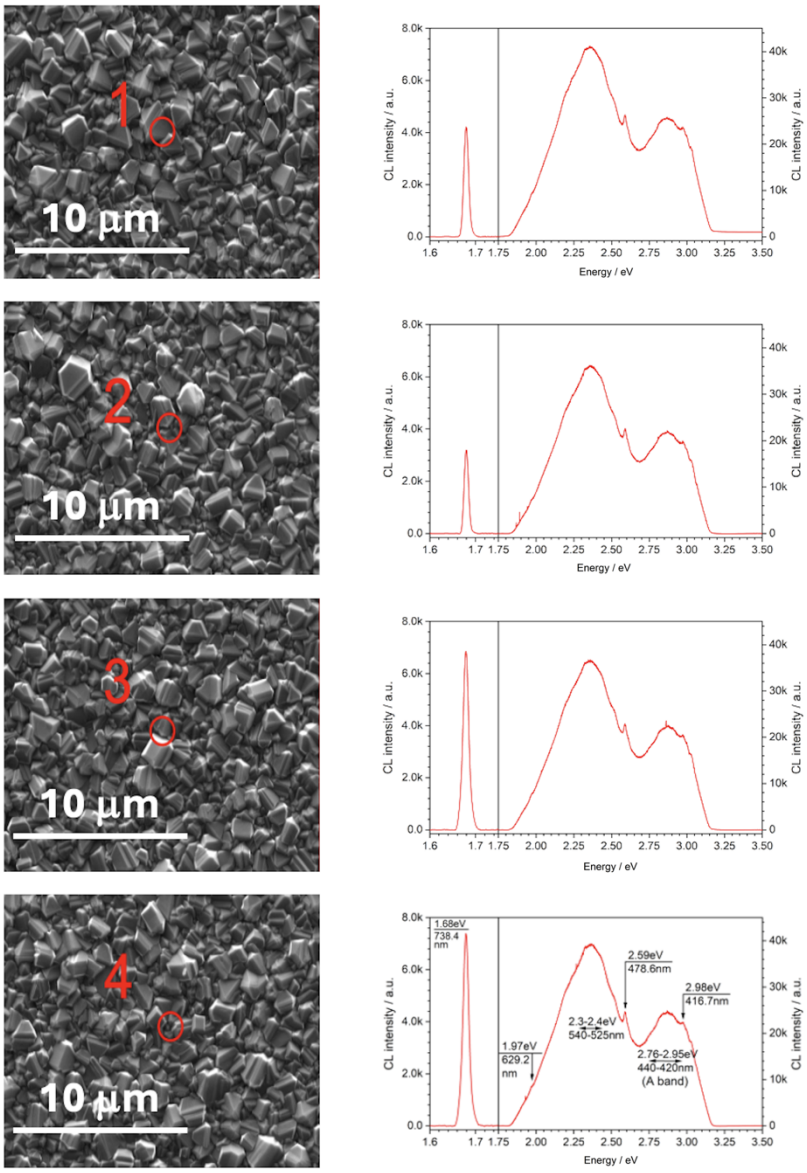

Figure S3. SEM images of sample S8 and CL spectra registered in the zone pointed out.

S5. Thermal relative sensitivity for the evaluation of thermometric descriptors extracted of the NV^- and SiV^- emission centers analyzed separately as a single signal

The relative thermal sensitivities (S_r) were calculated as performance parameter according to

$$S_r(\%) = \frac{1}{\Delta} \cdot \left|\frac{\delta\Delta}{\delta T}\right| \cdot 100 \qquad \text{(S1)}$$

where Δ are the thermometric descriptors depending on temperature, T. The relative thermal sensitivity was calculated for the three descriptors, area, intensity and FWHM, and for the ZPL emission of the NV- and SiV- centers. The results are shown in Figure S3. The highest thermal sensitivities were found for the SiV^- centers, considering the area and intensity, reaching a value of sensitivity by 4%.

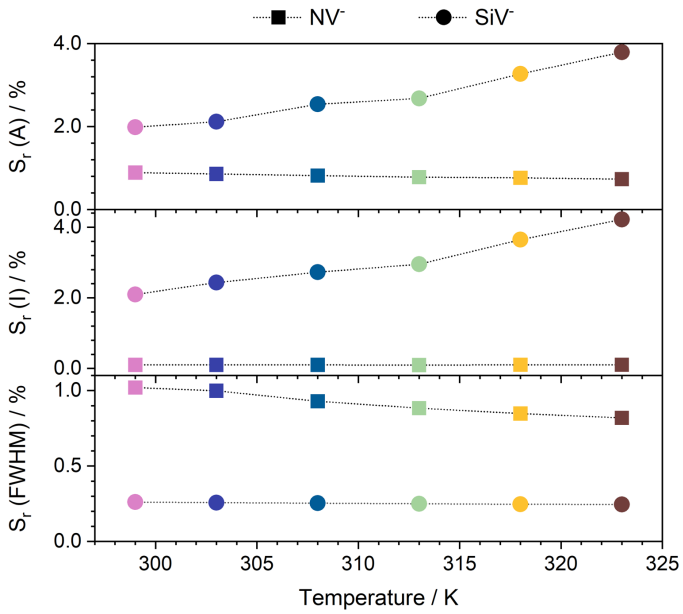

Figure S4. Relative thermal sensitivity obtained for the thermometric descriptors, area, intensity and FWHM, extracted of the NV^- and SiV^- emission centers analyzed separately as a single signal.